



Article

# Impact of Adsorption Layer Properties on Drainage Behavior of Microscopic Foam Films: The Case of Cationic/Nonionic Surfactant Mixtures

Dimi Arabadzhieva, Plamen Tchoukov and Elena Mileva \*

Institute of Physical Chemistry, Bulgarian Academy of Sciences, "Acad. G. Bonchev" Str. Bl. 11, 1113 Sofia, Bulgaria; dimi@ipc.bas.bg (D.A.); tchoukov@ipc.bas.bg (P.T.)

\* Correspondence: mileva@ipc.bas.bg

Received: 7 October 2020; Accepted: 11 November 2020; Published: 13 November 2020



**Abstract:** Aqueous mixtures of cationic hexadecyltrimethylammonium chloride (CTAC) and nonionic pentaethyleneglycol monododecyl ether ( $C_{12}E_5$ ) are investigated. Adsorption layer properties are systematically studied within a wide concentration range for a 1:1 molar ratio of the surfactants. Surface tension and dilatational rheology measurements are conducted by profile analysis tensiometry. The interfacial data are juxtaposed to drainage kinetics and stability results for microscopic foam films, investigated by microinterferometric thin liquid film instrumentation. The obtained results give experimental evidence of synergistic interactions in the studied solutions, as compared to the corresponding single surfactant systems. Specific runs of dynamic and equilibrium surface tension curves are registered against the total surfactant quantity; the surface dilatational elasticities for the mixtures are systematically higher. A clear correlation is established between adsorption layer performance and foam film characteristics. The maxima of the film lifetimes are well outlined, and the respective values are shifted towards lower overall concentrations. The reported results substantiate the key role of the adsorption layers, and the surface dilatational properties in particular, for foam film drainage kinetics and stability. The well-expressed synergy observed in adsorption layer and foam film properties suggests the substantial benefits of using mixed surfactant systems in the design and fine-tuning of foam systems for innovative applications.

**Keywords:** surfactant mixtures; foam films; adsorption; surface dilatational rheology; nonionic surfactants; cationic surfactants

## 1. Introduction

The onset of synergistic stabilization phenomena in aqueous systems containing low molecular mass (LMM) surfactant mixtures is a familiar phenomenon [1–4]. This synergy is closely related to the specific coupling of structure and properties' performance as compared to the single surfactant cases. One important aspect that is seldom studied in detail is the impact of the adsorption layer characteristics at the fluid interfaces on the drainage kinetics and stability of thin liquid films. The latter are essential structural components of foam systems, stabilized by LMM surfactants [5–7]. In our previous single-surfactant studies, it was clarified that equilibrium and dynamic surface tension isotherms might be correlated to the microscopic foam film's formation and stability [8–11]. We have found experimental evidence of the key role of the surface dilatational rheology, as well. These observations become possible because of the considerable advancements in profile analysis tensiometry (PAT) using oscillating bubbles/droplets [12,13], and the development of microscopic thin liquid instrumentation (TLF) [6,14,15].

Parallel studies of the adsorption layer's properties and the drainage kinetics of microscopic thin liquid films can provide a better understanding of foams stabilized by LMM surfactant mixtures.

The microinterferometric thin liquid film technique (TLF) has proven to be convenient instrumentation for model studies of dispersed systems, and of foams in particular [7,14,15]. One particular advantage is that the TLF setup allows well-controlled experimental conditions, and the precise determination of film lifetimes and critical thickness of rupture, which can be used to characterize the film stability.

The aim of the present paper is to explore the possible synergistic effects of the properties of the adsorption layers at the air interface, and the drainage behavior of foam films from aqueous solutions of cationic/nonionic surfactant mixtures. We have chosen the case of aqueous systems stabilized by hexadecyltrimethylammonium chloride (CTAC) and pentaethyleneglycol monododecyl ether ( $C_{12}E_5$ ). The surfactant choice is based on our previous studies of the single-surfactant cases [16,17]. The general outcome of these earlier studies has been the clearly observed concentration coincidence of the course of the film drainage characteristics, and the registered peculiarities of the adsorption layer's properties in relation to the surfactant concentration in each of the single-surfactant systems.

Here the results of a systematic study on the properties of aqueous solutions of mixtures of CTAC and  $C_{12}E_5$  at ambient temperature are presented. Extended data on the equilibrium and dynamic surface tensions and the dilatational viscoelastic moduli of the mixed surfactant systems are reported. Surface tension and dilatational rheology are established by profile analysis tensiometry in the regime of small-amplitude sinusoidal oscillations. The drainage and stability of microscopic foam films is investigated and juxtaposed to the performance of the adsorption layers at the solution/air interface. The aim is to investigate the specific conditions of possible synergetic effects, which may evidence the high potential of these mixed systems for further innovative applications.

## 2. Materials and Methods

### 2.1. Materials

Aqueous solutions containing mixtures of cationic surfactant hexadecyl trimethylammonium chloride (cetyltrimethyl ammonium chloride, CTAC, Fluka, 99.9% purity) and nonionic pentaethyleneglycol monododecyl ether ( $C_{12}E_5$ , Fluka, 98% purity, gas chromatography) were investigated. The overall surfactant concentration was in the range of  $1.0 \times 10^{-8}$ – $1.0 \times 10^{-4}$  mol/L. Sodium chloride (0.1 mol/L NaCl, Merk, 99.9% purity) was added to all solutions; it was heated beforehand at 600 °C for several hours to remove organic impurities. Triply distilled water (3D-water) with electrical conductivity 1.3 µS/cm was used; only in the case of the lowest surfactant concentrations was ultra-pure water from Sigma-Aldrich (CHROMASOLV® Plus, for HPLC) applied. The temperature during the experiments was kept constant at  $20 \pm 0.1$  °C.

### 2.2. Experimental Techniques

#### 2.2.1. Surface Tension and Dilatational Rheology of Air/Solution Surface

A profile analysis tensiometer (PAT-1, Sinterface) in the buoyant-bubble regime was applied to obtain dynamic and equilibrium surface tension values at the air/solution interface. The surface tension measurements were conducted until equilibrium values were achieved. The interfacial viscoelastic moduli were calculated using small-amplitude harmonic perturbations at the air/solution interface thereafter. The variations in the bubble surface area  $A$  led to changes in the surface tension values  $\gamma$  and the complex elasticity  $E$  was calculated as:  $E_{(iw)} = d\gamma/d\ln A$ . It is a function of the perturbation frequency  $w$ , and may be designated in terms of the surface dilatational elasticity ( $\varepsilon_d$ ) and surface dilatational viscosity ( $\eta_d$ ) of the perturbed interface [12,13]. The frequency of the bubble oscillations varied within the range of 0.005–0.2 Hz.

#### 2.2.2. Microinterferometric Thin Liquid Film Technique

Microscopic foam films were formed in a Scheludko-Exerowa cell [6,14,15]. Details on the experimental setup and procedures can be found elsewhere [6]. The capillary of the cell was filled

up with the aqueous solution and was equilibrated for 1 h. The liquid was then slowly withdrawn until a foam film was formed in the middle of the biconcave meniscus. The film was left to drain under the sucking action of the capillary pressure. The foam films were observed in reflected light with an inverted microscope Axiovert 200/MAT—Carl ZEISS, and recorded with a CCD video camera. Film-thickness values were extracted in the regime of monochromatic light (546 nm) using the method proposed by Scheludko and Platikanov [18]. The measuring cell was situated in a thermostatic chamber, and the temperature was kept at  $20 \pm 0.1$  °C using a Lauda thermostat (Ecoline E200 model).

### 3. Results and Discussion

The adsorption layer properties, and thin film drainage and stability, of single-surfactant aqueous solutions of C<sub>12</sub>E<sub>5</sub> and CTAC have been studied previously [16,17]. Some additional experiments with aqueous solutions of C<sub>12</sub>E<sub>5</sub> are added here, so as to complete the data for the single surfactant system. The major pool of data refers to 1:1 mol:mol ratio; several test experiments have also been done at mol:mol ratios of 1:10 and 10:1.

#### 3.1. Adsorption Layer Properties

##### 3.1.1. Dynamic and Equilibrium Surface Tension

The dynamic surface tension isotherms for mixed C<sub>12</sub>E<sub>5</sub>/CTAC (1:1 mol:mol ratio) are shown in Figure 1. Note that while there is a smooth decrease in the dynamic surface tension values within the concentration ranges of  $C_{\text{mix}} \sim 1.2 \times 10^{-8}$ – $5.0 \times 10^{-7}$  mol/L,  $C_{\text{mix}} \sim 2.0 \times 10^{-6}$ – $5.0 \times 10^{-6}$  mol/L and for  $C_{\text{mix}} \sim 1.0 \times 10^{-5}$ – $1.0 \times 10^{-4}$  mol/L, the run of the curve in the intermediate concentration domain  $C_{\text{mix}} = 1.0 \times 10^{-6}$  mol/L is quite irregular, and the surface tension values drop sharply, reaching values below those at higher concentrations ( $C_{\text{mix}} \sim 2.0$ – $5.0 \times 10^{-5}$  mol/L). This effect is most probably related to additional reorganization in the adsorption layer at the air/solution interface, and the onset of bulk premicellar self-assemblies.

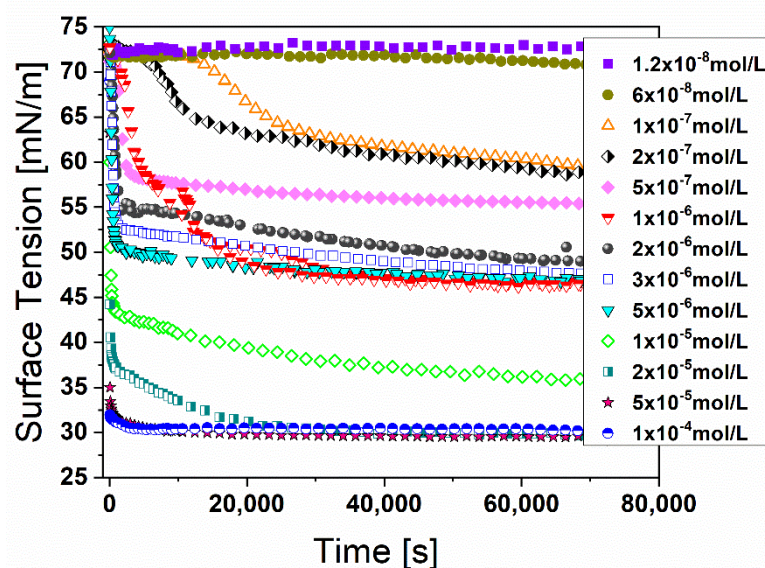


**Figure 1.** Dynamic surface tension curves of aqueous solutions of mixture C<sub>12</sub>E<sub>5</sub>/CTAC 1:1 for various total concentrations; 0.1 mol/L NaCl is added to all solutions and the temperature is 20 °C.

The experimental results for the equilibrium surface tensions of the mixed 1:1 C<sub>12</sub>E<sub>5</sub>/CTAC aqueous solutions are shown in Figure 2. The criterion for reaching surface tension equilibrium is that the measured values remain constant (within  $\pm 0.1$  mN/m) for at least 1 h. Previously obtained data [16,17] are also shown in Figure 2 for comparison. The basic characteristics of the equilibrium

surface tension curve are similar to those of the single-surfactant cases, including the presence of a premicellar plateau region for the intermediate concentrations. It should be mentioned that in the mixed solution, this plateau extends within the range of  $1 \times 10^{-6}$  mol/L to  $5 \times 10^{-6}$  mol/L, partially embracing the respective values of the premicellar regions in the single-surfactant cases ( $2 \times 10^{-7}$  mol/L to  $1 \times 10^{-6}$  mol/L for  $C_{12}E_5$ , and  $2 \times 10^{-6}$  mol/L to  $5 \times 10^{-6}$  mol/L for CTAC). This might be interpreted as additional experimental evidence for the formation of bulk premicellar aggregates, most probably being composed from surfactant molecules of one type—initially  $C_{12}E_5$  premicelles appear, and then CTAC premicelles start to form. Besides this, the onset of the premicellar plateau region is in conformity with the registered irregular run of the dynamic surface tension curve at  $C_{\text{mix}} = 1.0 \times 10^{-6}$  mol/L (Figure 1). The sharp drop in the equilibrium surface tension value at this  $C_{\text{mix}}$  value might be interpreted as the onset of a short concentration interval, where the adsorption of single surfactant molecules at the air/solution interface is prevailing over the bulk premicellization process.

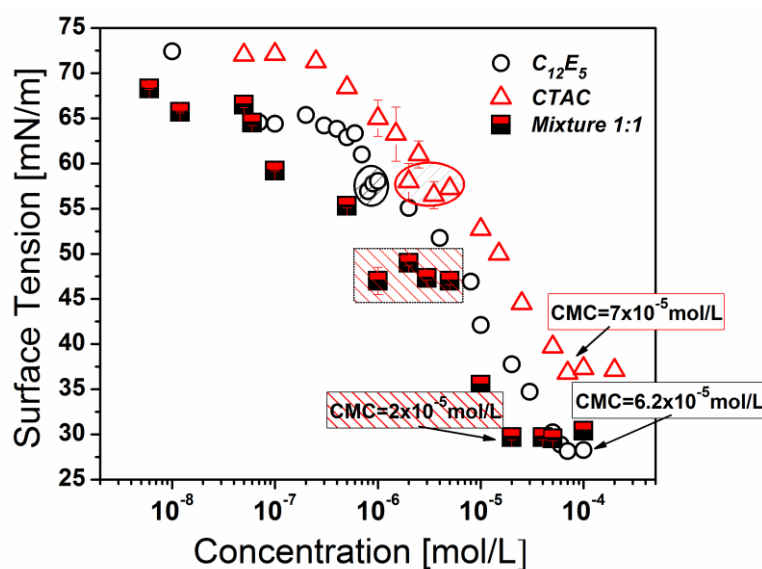


**Figure 2.** Equilibrium surface tension isotherms of aqueous solutions of 1:1 mixture  $C_{12}E_5$ /CTAC and of single surfactants CTAC and  $C_{12}E_5$ ; 0.1 mol/L NaCl is added to all solutions and the temperature is 20 °C.

The critical micelle concentration ( $\text{CMC}_{\text{mix}}$ ) value for the mixed system is  $2.0 \times 10^{-5}$  mol/L, which is approximately three times lower than the respective CMCs of the single surfactant solutions ( $7.0 \times 10^{-5}$  mol/L for CTAC and  $6.2 \times 10^{-5}$  mol/L for  $C_{12}E_5$ ). The equilibrium surface tension values of the mixed system are lower than both the respective values of the cationic surfactant and the nonionic single surfactant within most of the total concentration range. However, the final surface tension value for the mixed system at  $\text{CMC}_{\text{mix}}$  (29.7 mN/m) is quite near the CMC of the nonionic single-surfactant case (28.8 mN/m). These peculiarities indicate strong synergy in the mixed surfactant system, and might be regarded as experimental evidence of the formation of mixed micellar aggregates and mixed adsorption layer coverage.

### 3.1.2. Surface Dilatational Rheology

The results for the surface dilatational elasticities ( $\varepsilon_r$ ) of the adsorption layers at the air/solution interface in the mixed  $C_{12}E_5$ /CTAC system, at oscillation frequencies in the interval 0.005–0.2 Hz, are presented in Figure 3a. A specific tendency in the run of the curves should be noted. While at very low total surfactant concentrations ( $C_{\text{mix}} < 1.0 \times 10^{-7}$  mol/L) the elasticity values are lower than in the respective single-surfactant cases, they enhance dramatically in the mixed systems upon the increase in the surfactant quantity passing through one high maximum ( $C_{\text{mix}} = 1.0 \times 10^{-6}$  mol/L,  $\varepsilon_r \sim 90$ –115 mN/m, within the whole frequency range) and one lower maximum ( $C_{\text{mix}} = 1.0 \times 10^{-5}$  mol/L,  $\varepsilon_r \sim 35$ –73 mN/m),

and then decline sharply at higher total concentrations above  $\text{CMC}_{\text{mix}}$ . When comparing with the equilibrium surface tension data in Figure 2, one could notice that the first concentration range pertains to the premicellar plateau—for these solutions, the surface dilatational elasticity is considerably higher and there is a clear dependence on the oscillation frequencies. This supports the hypothesis that premicellar self-assemblies might appear in the bulk of the solution, consuming the added amphiphile quantities. The juxtaposition of Figures 2 and 3a also indicates that possible premicellar aggregates might be composed predominantly of one type of LMM surfactant, while the adsorption layer should be a mixture of both surfactants. The surface dilatational viscosities remain relatively low, and the concentration dependence does not change significantly within the whole investigated domain compared to the single-surfactant cases (Figure 3b). Only the maximum values are shifted towards higher  $C_{\text{mix}}$ .

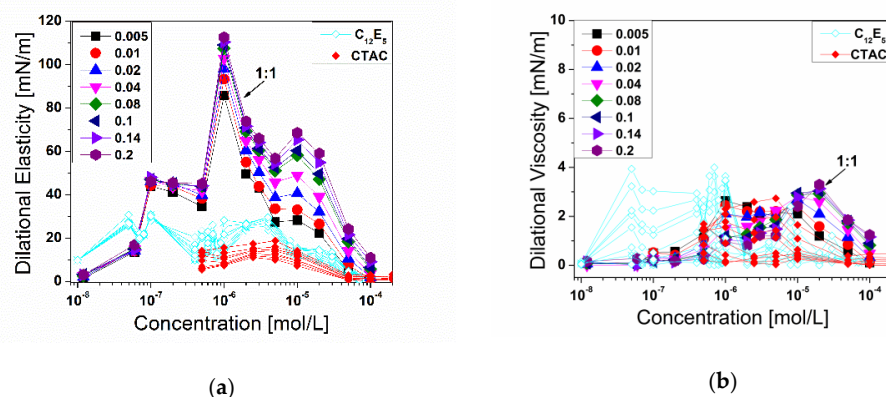


**Figure 3.** Surface dilatational moduli of aqueous solutions of mixture  $\text{C}_{12}\text{E}_5/\text{CTAC}$  1:1 (in the presence of 0.1 M NaCl and at temperature  $t = 20^\circ\text{C}$ ) as a function of the total surfactant concentration and the frequency of oscillations. (a) The dilatational elasticity of the mixed system is given as solid symbols. The open symbols represent single surfactants systems reported before in references [16,17]. (b) Surface dilatational viscosity of the mixed system.

The complex interplay of surfactant mass transfer between the bulk of the solutions and the adsorption layer is further clarified by experiments applying different time periods of initial incubation before the start of the dilatational rheology studies. A detailed depiction of the evolution of the surface dilatational elasticity against the oscillation frequencies for various  $C_{\text{mix}}$  is presented in Figure 4.

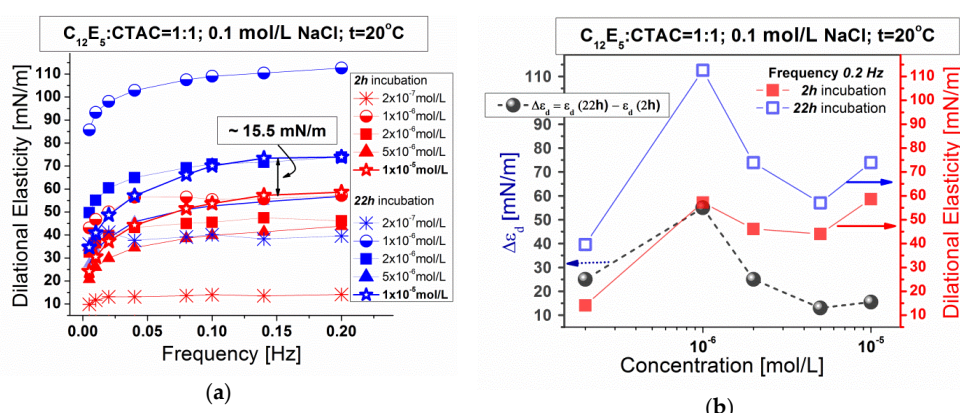


**Figure 4.** Evolution of dilatational elasticity values. (a) Frequency dependence of dilatational elasticity at two different ageing times of the adsorption layers—after 2 h (red symbols) and 22 h (blue symbols) from the beginning of the formation of the fresh surface. (b) Dilatational elasticity for 0.2 Hz frequency as a function of surfactant concentration after 2 h (red symbols) and 22 h (blue symbols).

To summarize, the adsorption layer studies show a well-defined tendency of increase in the surface dilatational values when the solution incubation period is enhanced from 2 to 22 h. The trend is valid for all applied oscillation frequencies and for all total surfactant concentrations of the aqueous solution mixtures. The most noteworthy effect is observed for the intermediate concentration of  $C_{\text{mix}} = 1.0 \times 10^{-6}$  mol/L, where the peak in the difference  $\Delta\varepsilon_d = \varepsilon_d(22 \text{ h}) - \varepsilon_d(2 \text{ h})$  is registered. This coincides with the start of the first (premicellar) plateau in the surface tension isotherm (Figure 2). The obtained results, together with the data for the dynamic surface tension in Figure 1, confirm once more that the probable onset of premicellar self-assemblies leads to specific rearrangements in the adsorption layers, as well.

### 3.2. Microscopic Foam Film's Drainage Characteristics

The microscopic foam film experiments were performed with mixed CTAC/C<sub>12</sub>E<sub>5</sub> systems of three mol:mol ratios: 1:1, 1:10 and 10:1. All films are unstable, with drainage passing through various stages, and rupture within 1–2 min. Besides, at surfactant concentrations  $C_{\text{mix}} > 1.0 \times 10^{-6}$  mol/L, technical difficulties are encountered in forming the film in a common Scheludko–Exerowa cell. This is most probably related to the poor wetting conditions on the glass capillary surface. So, the foam films from aqueous solutions of  $C_{\text{mix}} > 1.0 \times 10^{-6}$  mol/L are obtained on a porous plate cell. The film thickness values, just before rupture for different concentrations of the 1:1 CTAC/C<sub>12</sub>E<sub>5</sub> system, are presented in Figure 5. Test results for the 1:10 and 10:1 CTAC/C<sub>12</sub>E<sub>5</sub> solutions are also included.

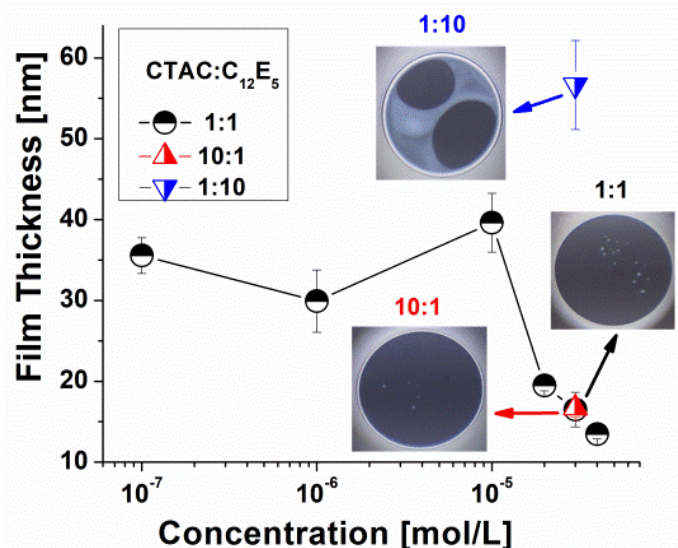


**Figure 5.** Critical film thicknesses of aqueous solutions of mol:mol = 1:1 CTAC/C<sub>12</sub>E<sub>5</sub> mixtures against the total surfactant concentration ( $C_{\text{mix}}$ ). The films rupture at thickness in the range of 17–40 nm. Test values for the 1:10 and 10:1 CTAC/C<sub>12</sub>E<sub>5</sub> solutions at  $C_{\text{mix}} = 3.0 \times 10^{-5}$  mol/L are presented.

Typical snapshots from the evolution of a foam film obtained from the CTAC/C<sub>12</sub>E<sub>5</sub> mixture (1:1) at the total surfactant concentration of  $3.0 \times 10^{-5}$  mol/L, which is above the  $\text{CMC}_{\text{mix}}$  ( $2.0 \times 10^{-5}$  mol/L), are shown in Figure 6. Three well-distinguished thickness regions are observed: background black regions with thickness  $\sim 20$  nm, darker black spots with thickness  $\sim 17$  nm, and white dots. The latter represent film portions of a higher thickness. The white dots usually move slowly within the film, coalesce upon contact, and disappear via draining slowly into the surrounding thinner regions.

Exemplary snapshots of film drainage in the cases of the 1:10 and 10:1 CTAC/C<sub>12</sub>E<sub>5</sub> mixtures at  $C_{\text{mix}} = 3.0 \times 10^{-5}$  mol/L are shown in Figure 7. In the case of 1:10 CTAC/C<sub>12</sub>E<sub>5</sub>, the formation of black spots in the films is well detected (Figure 7a). These films rupture before the moment when the black spots embrace the whole film area to form black films. In the case of 10:1 CTAC/C<sub>12</sub>E<sub>5</sub> (Figure 7b), the qualitative observations are formally similar to those for 1:1 CTAC/C<sub>12</sub>E<sub>5</sub> (compare with

Figure 6). Two different thickness regions—background black film and white dots—are also recorded. Although the film lifetimes are slightly longer, the films finally rupture in about 1–2 min.

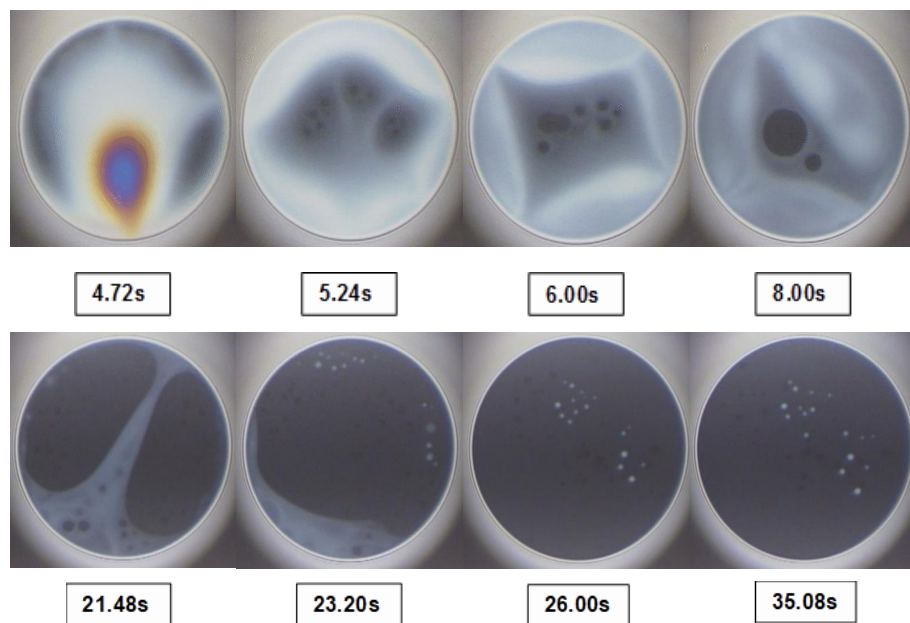


**Figure 6.** Evaluation of drainage of foam film stabilized for total surfactant concentration  $3.0 \times 10^{-5}$  mol/L of the mixture CTAC/C<sub>12</sub>E<sub>5</sub>, mol:mol = 1:1. The foam films drain and rupture. Two regions of thickness and white dots are registered. The overall thickness in the last snapshot is ~20.4 nm for the homogeneous portion of the film and ~16.8 nm for the black spots.

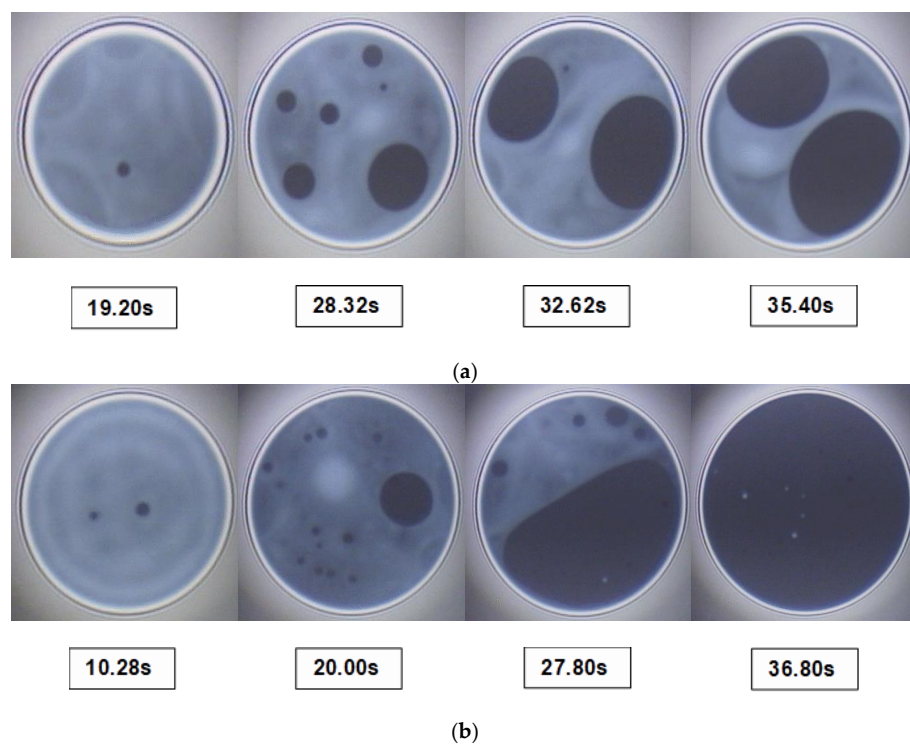


**Figure 7.** Evaluation of drainage of foam film stabilized for total surfactant concentration  $3.0 \times 10^{-5}$  mol/L of the mixture. (a) CTAC:C<sub>12</sub>E<sub>5</sub> = 1:10. The foam films drain and rupture before the onset of black films. There are no white dots. (b) CTAC:C<sub>12</sub>E<sub>5</sub> = 10:1. Two regions of thickness and white dots are formed, but their number is notably less than in Figure 6.

In the film experiments at a higher total concentration— $C_{\text{mix}} = 4 \times 10^{-5} \text{ mol/L} = 2 \times \text{CMC}_{\text{mix}}$ —white spots and black spots are simultaneously formed (Figure 8). The white spots quickly merge with each other, reducing their total number as compared with the foam films at the lower concentration (compare Figures 6 and 8), and the larger white spots quickly ‘dissolve’ within the thinner portions of the films. The respective black dots and spots also quickly merge with each other, enlarge, and embrace the whole film area. The final outcome is an unstable black film of homogeneous thickness, which finally ruptures in less than 2 min.

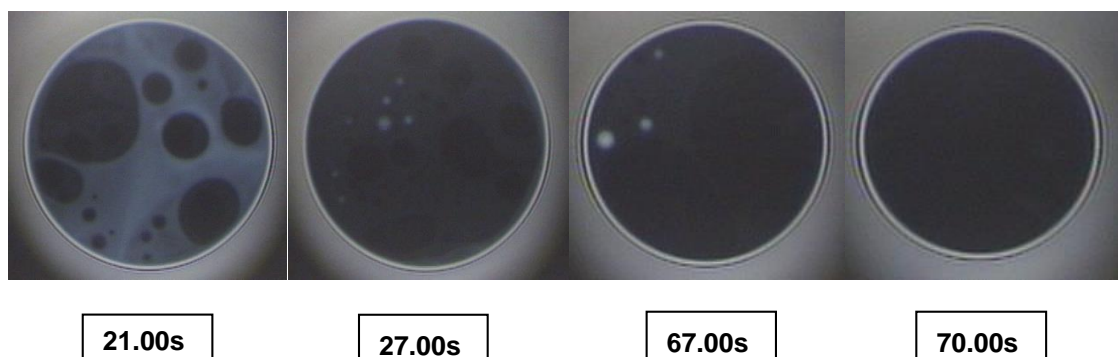


**Figure 8.** Evaluation of drainage of foam film stabilized for total surfactant concentration  $4 \times 10^{-5}$  mol/L of the CTAC:C<sub>12</sub>E<sub>5</sub> = 1:1 mixture.

#### 4. Discussion

The obtained results for the properties of the mixed CTAC/C<sub>12</sub>E<sub>5</sub> aqueous solutions at ambient temperatures support the idea about the significant synergistic interactions of the LMM surfactants. The synergy is made evident by the following experimental outcomes:

1. The surface tension data, both dynamic and equilibrium, are generally lower than the values for the single-surfactant aqueous solutions. The only exception is for  $C_{\text{mix}} \geq \text{CMC}_{\text{mix}}$ ;
2. The data for the surface dilatational elasticities are considerably higher than in the single-surfactant aqueous solutions, at the same molar concentrations, as the maxima are shifted toward lower  $C_{\text{mix}}$ . The surface dilatational viscosities are of the same order of magnitude as in the single-surfactant cases, as the maxima are shifted toward higher  $C_{\text{mix}}$ ;
3. While the microscopic foam films obtained from aqueous solutions of single surfactants reach equilibrium states at higher concentrations (at and above the respective CMCs), all films studied here are unstable, with drainage passing through various stages, and rupture within 1–2 min for the whole concentration range, even at  $C_{\text{mix}} = 2 \times \text{CMC}_{\text{mix}}$ .

From the surface tension isotherms, as presented in Figure 2, and insofar as the mol:mol ratio is 1:1, one might presume that the impact of the nonionic surfactant (C<sub>12</sub>E<sub>5</sub>) is generally stronger than that of the cationic substance (CTAC). One possible reason is that the area of the head group of C<sub>12</sub>E<sub>5</sub> might be larger compared to that of CTAC, and therefore a lower number of molecules could ensure the same adsorption layer coverage. To investigate this notion more deeply, the effect of the order of single-surfactant addition on the interfacial properties is explored. The total surfactant concentration is  $C_{\text{mix}} = 1.0 \times 10^{-6}$  mol/L, where the onset of bulk premicellar self-assemblies is anticipated. First, a “premixed” approach is used, in which the two surfactants are simultaneously added to water in the ratio 1:1 (mol:mol). They are fully dissolved before the formation of the fresh air/solution interface (bubble) in the PAT setup, and surface tension measurements and the extraction of interfacial rheological parameters are performed thereafter. Second, the following “supplement” procedure is executed: (1) a solution of one of the surfactants, C<sub>12</sub>E<sub>5</sub> or CTAC, is prepared using half of the targeted total surfactant concentration; (2) a fresh bubble is formed in the PAT cuvette, and dynamic interfacial tension is measured until the equilibrium values are attained; (3) an aqueous solution of the second

surfactant, with half of the targeted total surfactant concentration, is added carefully to the cuvette until the acquisition of the desired total amphiphile quantity; (4) dynamic surface tension is recorded until equilibrium values are reached. Then, bubble surface area oscillations are measured, and the rheological parameters for the adsorption layer at the air/solution interface are extracted. Provided the final chemical composition of the system is the same under equilibrium conditions, the properties of the surface layers might be expected to be the same as well. However, the kinetics of the formation of the adsorption layers turns out to be different, and it strongly depends on the order of adding the surfactants. The results of the “premixed” and “supplement” methods are shown in Figure 9.

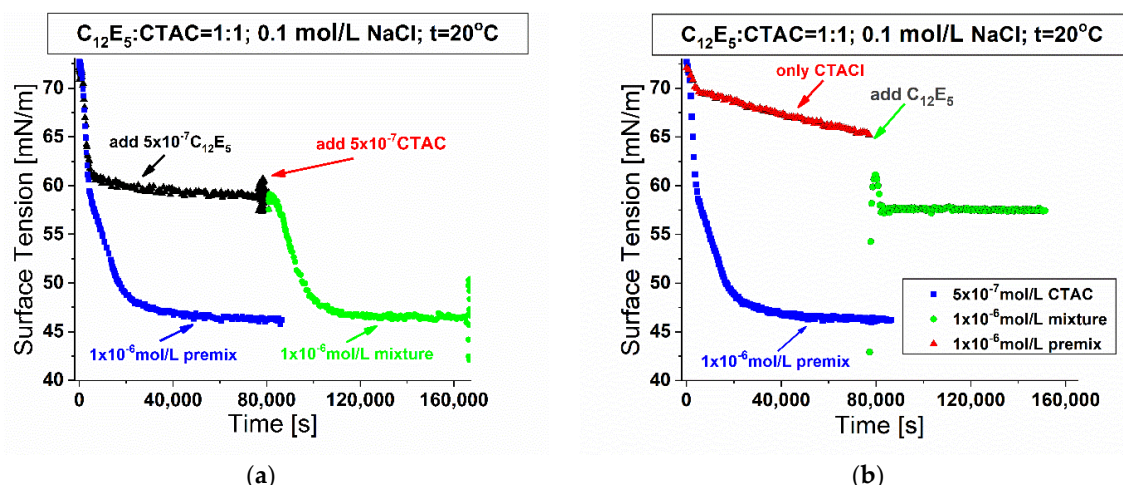


**Figure 9.** Dynamic surface tension isotherms of “premixed” and “supplement method” surfactant solutions. Final solutions are 1:1 mixtures with total surfactant concentration  $1.0 \times 10^{-6}$  mol/L. (a) CTAC solution is added to the previously obtained  $C_{12}E_5$  system; (b)  $C_{12}E_5$  solution is added to the previously obtained CTAC system.

As is to be seen, the mixing sequence significantly influences the final equilibrium data of the system. If one starts with the aqueous system of  $C_{12}E_5$  and thereafter adds a solution of CTAC, the equilibrium surface tension reaches the same value as for the “premixed” case (Figure 9a). The reversed sequence of addition (first start with CTAC solution and then add the solution of  $C_{12}E_5$ ) results in a higher final equilibrium surface-tension value, namely 57.5 mN/m, as compared to 46.2 mN/m for the “premixed” system (Figure 9b). Besides, the run of the dynamic surface tension against the surfactant concentration for the CTAC-only solution is much smoother than in the “premixed” system. When the second component ( $C_{12}E_5$ ) is introduced, there is an almost immediate additional drop in the surface tension, and the final equilibrium value is quickly attained. The surface tension curves are not entirely reproducible in this case, and the experiment has been repeated three times. Regardless, the final equilibrium surface tension value is considerably higher than the respective value for the “premixed” case. These results presume that the adsorption layer coverage in a regime below  $CMC_{mix}$  is dominated by the nonionic substance ( $C_{12}E_5$ ).

The interfacial dilatational elasticities for the mixed systems are higher as compared to the single-surfactant cases (Figure 3a). These results also depend on the sequence of adding the surfactant (Figure 10). Thus the interfacial dilatational elasticities of the nonionic surfactant solution ( $C_{12}E_5$ ), following the addition of CTAC, are the same as in the “premixed” case, while for the reversed order of addition—taking the CTAC solution and adding the  $C_{12}E_5$  solution—the values are significantly different.

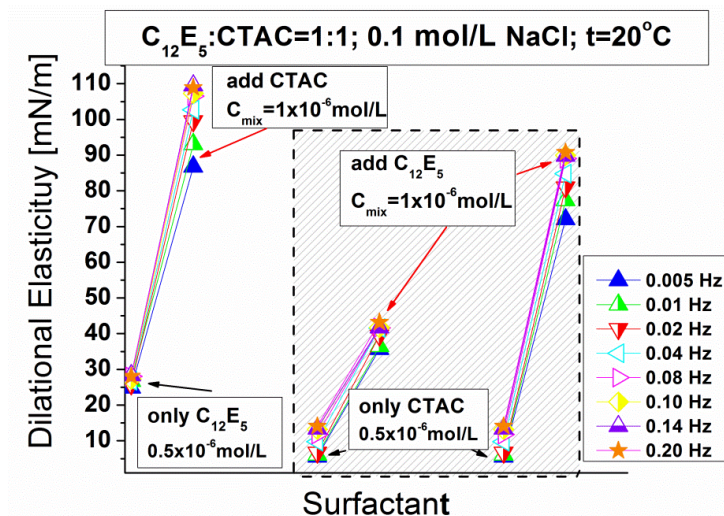


**Figure 10.** Dilatational elasticity change after addition of second component:  $C_{12}E_5$  is added to existing CTAC adsorption layer and CTAC addition to  $C_{12}E_5$  adsorption layer; the final solutions are 1:1 mixtures with total surfactant concentration's  $1.0 \times 10^{-6}$  mol/L.

Here it should be remembered that the dilatational elasticity of the mixed system changes significantly when the surface is aged up to 22 h (Figures 3a and 4). This result signifies that the time evolution of the adsorption and rheological properties of the mixed cationic/nonionic surfactants' adsorption layers have to be considered. Juxtaposed with the outcome that the final (time interval up to 160,000 s) state of the adsorption layer of the mixed systems in the intermediate concentration region depends on the order of addition of the surfactants, this is an interesting result that needs further investigation.

The “supplement” method is also tested for a higher total surfactant concentration of the mixed system ( $C_{\text{mix}} = 4.0 \times 10^{-5}$  mol/L =  $2 \times \text{CMC}_{\text{mix}}$  (Figure 11)). The main outcome in this case is that the order of surfactant addition is not important for the final value of the surface tension of the mixed solution. Moreover, the dilatational elasticities are also independent of the specific order of adding the single surfactant to the aqueous solution of the other surfactant (Figure 12).

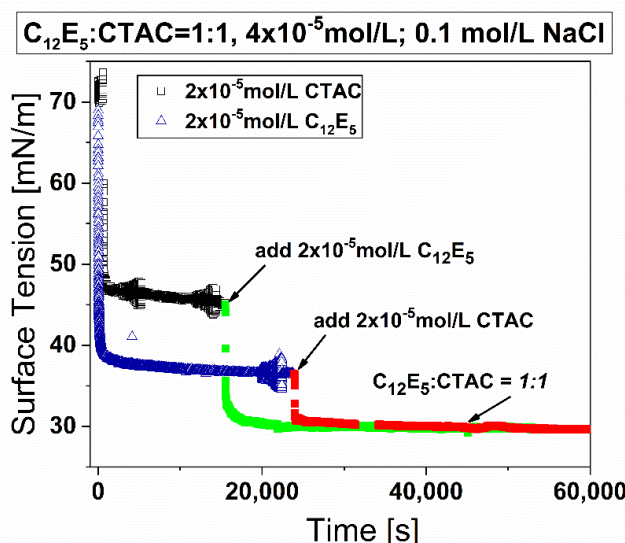


**Figure 11.** Dynamic surface tension of a single component and consecutive addition of second component. The total surfactant concentration is  $4.0 \times 10^{-5}$  mol/L for mol:mol ratio of 1:1 mixture CTAC and  $C_{12}E_5$ .

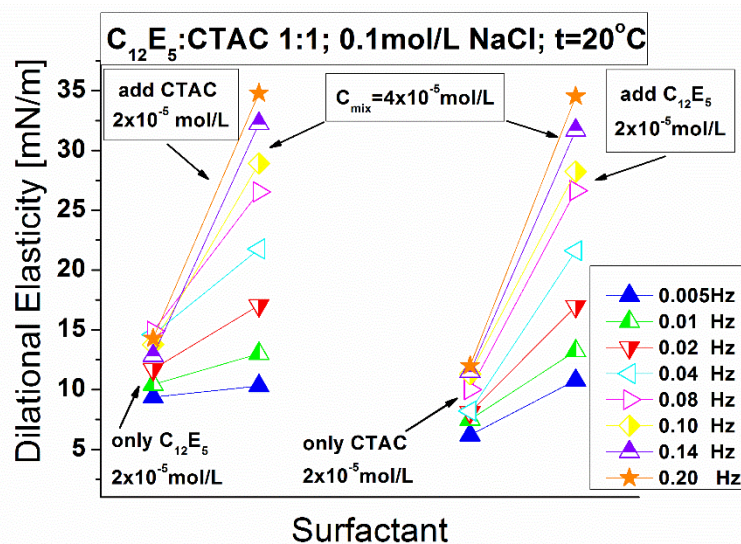


**Figure 12.** Dilatational elasticity change after addition of second component:  $C_{12}E_5$  is added to existing CTAC adsorption layer; CTAC addition to  $C_{12}E_5$  adsorption layer; final mol:mol ratio is 1:1 for the mixture with total surfactant concentration of  $4.0 \times 10^{-5}$  mol/L.

These test experiments shed additional light on the details of the synergy between the two surfactants. While the total concentration is below that of the single-surfactant CMCs, the nonionic species ( $C_{12}E_5$ ) seems to be more effective regarding its role in the structure-formation of the adsorption layer at the air/solution interface. This might be related to the larger hydrophilic portion of  $C_{12}E_5$ . In the case of CTAC, and in the presence of added NaCl, the hydrophilic head group is smaller and the decrease in surface tension might be less for the same single-surfactant concentrations. Besides, the “supplement” method displays more clearly that  $C_{12}E_5$  premicelles might appear first, before CTAC premicelles. However, at concentrations higher than  $CMC_{mix}$ , the equilibrium surface tension value is the same as in the “premixed” case, and does not depend on the order of mixing the surfactants. Here, the lack of effect on the surface dilatational elasticities and the overall lower elasticity values could indicate the completion of the structure of the mixed adsorption layer and the formation of bulk self-assemblies, which are most probably mixed micelles.

The foam film drainage and stability are in synchrony with the changes in the adsorption layer’s properties as related to the surfactant concentration ( $C_{mix}$ ). The qualitative picture of the draining films is characterized by the onset of white spots and black formations (dots and spots). These peculiarities are well-known from the single-surfactant cases of aqueous solutions derived from LMM surfactants. The local minimum in the film thickness values at  $C_{mix} = 1.0 \times 10^{-6}$  mol/L (Figure 5) coincides with both the start of the premicellar portion of the surface tension isotherm (Figure 2) and the maximum of the surface dilatational elasticity (Figure 3a). Insofar as the foam films drain via a regime of high interfacial mobility, the partial stabilization of the foam film’s drainage is most probably due to the Marangoni effect, related to the decomposition of the existing premicelles in the film bulk. The details of this partial stabilization are experimentally verified for single-surfactant cases [16,17,19–22]. At higher  $C_{mix}$ , but below  $CMC_{mix}$ , this effect is complicated due to the continuous preferential adsorption of the nonionic surfactant. The result is an increase in the critical film thickness of rupture. Here, although the nonionic  $C_{12}E_5$  is more efficient in adsorbing at the interface and reducing the surface tension, the relatively large hydrophilic portions of these molecules prevent them from forming well-packed adsorption layers. This is additionally verified by the much larger film thickness in the case of CTAC ( $C_{12}E_5 = 1:10$ ) (see also Figure 5).

At sufficiently high concentrations ( $C_{mix} \geq CMC_{mix}$ ), the films can drain up to much lower thickness values (~17 nm). It is presumed that a mixed adsorption layer is formed. The inclusion of additional CTAC molecules partially stabilizes the foam films. The mechanism of stabilization

might be also related to the increase in the surface charge at the film interface, causing the onset of positive electrostatic disjoining pressure. It should be noted that in the presence of a greater CTAC quantity (CTAC:C<sub>12</sub>E<sub>5</sub> = 10:1), the film snapshots (Figure 7a) and the critical film thickness (~17 nm) are actually the same as in the equimolar mixture (CTAC:C<sub>12</sub>E<sub>5</sub> = 1:1, Figure 5). On the contrary, if CTAC:C<sub>12</sub>E<sub>5</sub> = 1:10, the critical film thickness is approximately three times higher (~55 nm, Figure 5). The appearance of considerable numbers of white spots could be due to the presence of larger mixed micelles in the film bulk, which are squeezed out in the thinner (black) portions of the film and in the meniscus, allowing the formation of (almost) homogeneous, but unstable, black films.

In overall, the obtained experimental data evidence the complex mechanisms of the synergistic interactions and reorganizations occurring within the adsorption layer at the air/solution interface, in the solution bulk, and in the confined space of the microscopic foam films. They give additional basis for the further development of finely tuned conceptual models and theoretical approaches. According to the known general theoretical scheme for mixed systems [23], the results in the present study presume that, at least for the aqueous mixture of these particular types of LMM surfactants, the ideal behavior and the antagonism should be excluded. However, the various aspects of synergy reported here might be related to some of the developed models for adsorption layer formation and performance, as in [24], combined with the theoretical analyses on the possible formation of single LMM and mixed bulk self-assemblies, as in [25]. Regardless, the well-outlined premicellar and micellar concentration domains in the investigated aqueous solutions have to be accounted for.

## 5. Conclusions

The reported experimental results concerning the surface tension, surface dilatational rheology and foam film drainage and stability give grounds for the advancement of the following hypothesis:

In aqueous solutions of the particular LMM nonionic/cationic surfactant mixture (C<sub>12</sub>E<sub>5</sub> and CTAC), and within the whole investigated concentration range, several specific peculiarities may be evidenced. These are as follows:

- At low concentrations, the nonionic C<sub>12</sub>E<sub>5</sub> performs as a more surface-active species than CTAC;
- Within the intermediate concentration domain, premicellar entities are formed. Most probably, these premicelles appear consecutively, with the onset of nonionic and then ionic self-assemblies. These species are built up of single LMM surfactants;
- The adsorption layer is composed of a mixture of the LMM surfactants. The layer is not very tightly packed;
- At C<sub>mix</sub> ≥ CMC<sub>mix</sub>, mixed bulk micelles are formed, and these might be more stable than the single-surfactant micelles;
- CTAC presumably plays a more significant role in the control over foam film thickness and stability. This effect is most likely due to the cationic nature of CTAC and the initiation of electrostatic disjoining pressure in the film.

The outcomes from the present study substantiate the key role of the adsorption layers, and the surface dilatational properties in particular, in foam film drainage kinetics and stability. The well-expressed synergy observed in the adsorption properties and foam film performance suggests the substantial benefits of using mixed surfactant systems in the design and fine-tuning of foam systems for innovative applications.

It should be mentioned that, unlike mixtures of cationic/anionic, anionic/nonionic, etc., surfactants, the cases of LMM cationic/nonionic amphiphiles are not so often systematically investigated, particularly in view of the properties and stability of foam systems. However, such types of LMM surfactant mixtures are components of various formulations intended to be applied in different industrial fields, for example gas injection for enhanced oil recovery [26], household cleansing [27,28], etc. Through the choice of appropriate substances, suitable composition ratios, and the addition of specific additives, the usage of such formulations may be further optimized. The data presented here provide experimental

evidence that knowledge about the specific interactions of the LMM surfactants in the mixture, and an outline of the conditions for well-expressed synergy as compared to the single-surfactant cases, are key bases for the well-focused fine-tuning of foam formulations. Therefore, the detailed study of this synergy and the associated system's performance are of primary importance for specific applications.

**Author Contributions:** Conceptualization, D.A., P.T., E.M.; methodology, D.A., P.T., E.M.; formal analysis, D.A., P.T., E.M.; investigation, D.A.; resources, D.A., E.M.; data curation, E.M.; writing—original draft preparation, D.A., P.T.; writing—review and editing, E.M. All authors have read and agreed to the published version of the manuscript.

**Funding:** This research received no external funding.

**Conflicts of Interest:** The authors declare no conflict of interest.

## References

1. Fainerman, V.B.; Lucassen-Reynders, E.H. Adsorptions of single and mixed ionic surfactants at fluid interfaces. *Adv. Colloid Interface Sci.* **2002**, *96*, 295–323. [[CrossRef](#)]
2. Aksenenko, E.V.; Kovalchuk, V.I.; Fainerman, V.B.; Miller, R. Surface dilational rheology of mixed surfactants layers at liquid interfaces. *J. Phys. Chem. C* **2007**, *111*, 14713–14719. [[CrossRef](#)]
3. Penfold, J.; Thomas, R.K. Mixed surfactants at the air-water interface. *Annu. Rep. Prog. Chem. Sect. C* **2010**, *106*, 14–35. [[CrossRef](#)]
4. Fainerman, V.B.; Aksenenko, E.V.; Mys, A.V.; Petkov, J.T.; Yorke, J.; Miller, R. Adsorption layer characteristics of mixed SDS/C<sub>n</sub>EO<sub>m</sub> solutions. 3. Dynamics of adsorption and surface dilational rheology of micellar solutions. *Langmuir* **2010**, *26*, 2424–2429. [[CrossRef](#)] [[PubMed](#)]
5. Scheludko, A. Thin liquid films. *Adv. Colloid Interface Sci.* **1967**, *1*, 391–464. [[CrossRef](#)]
6. Exerowa, D.; Kruglyakov, P.M. *Foam and Foam Films*; Elsevier Science B.V: New York, NY, USA, 1998; pp. 1–344.
7. Khristov, K. Role of foam films in foam stability. In *Foam Films and Foams*; Progress in Colloid and Interface Science; Exerowa, D., Gochev, G., Platikanov, D., Liggieri, L., Miller, R., Eds.; CRC Press: Boca Raton, FL, USA, 2019; pp. 233–243.
8. Tchoukov, P.; Mileva, E.; Exerowa, D. Drainage time peculiarities of foam films from amphiphilic solutions. *Colloids Surf. A* **2004**, *238*, 19–25. [[CrossRef](#)]
9. Mileva, E.; Tchoukov, P.; Exerowa, D. Amphiphilic nanostructures in thin liquid films. *Adv. Colloid Interface Sci.* **2005**, *114*, 47–52. [[CrossRef](#)] [[PubMed](#)]
10. Mileva, E.; Exerowa, D. Amphiphilic nanostructures in foam films. *Curr. Opin. Colloid Interface Sci.* **2008**, *13*, 120–127. [[CrossRef](#)]
11. Mileva, E. Impact of adsorption layers on thin liquid films. *Curr. Opin. Colloid Interface Sci.* **2010**, *15*, 315–323. [[CrossRef](#)]
12. Loglio, G.; Pandolfini, P.; Miller, R.; Makievski, A.V.; Ravera, F.; Ferrari, M.; Liggieri, L. Drop and Bubble Shape Analysis as Tool for Dilational Rheology Studies of Interfacial Layers. In *Novel Methods to Study Interfacial Layers*; Studies in Interface Science; Möbius, D., Miller, R., Eds.; Elsevier: Amsterdam, The Netherlands, 2001; Volume 11, pp. 439–483.
13. Miller, R.; Olak, C.; Makievski, A.V. Tensiometry as a tool for quantitative analysis of surfactant adsorption. *SÖFW J.* **2004**, *130*, 2–10.
14. Platikanov, D.; Exerowa, D. Thin liquid films. In *Fundamentals of Interface and Colloid Science*; Lyklema, H., Ed.; Academic Press: London, UK, 2005; Volume 5, pp. 1–91.
15. Platikanov, D.; Exerowa, D. Fundamentals of foam films. In *Foam Films and Foams*; Progress in Colloid and Interface Science; Exerowa, D., Gochev, G., Platikanov, D., Liggieri, L., Miller, R., Eds.; CRC Press: Boca Raton, FL, USA, 2019; pp. 77–98.
16. Arabadzhieva, D.; Tchoukov, P.; Mileva, E.; Miller, R.; Soklev, B. Impact of amphiphilic nanostructures on formation and rheology of adsorption layers and on foam film drainage. *Ukr. J. Phys.* **2011**, *58*, 801–810.
17. Arabadzhieva, D.; Tchoukov, P.; Soklev, B.; Mileva, E. Interfacial layer properties and foam film drainage kinetics of aqueous solutions of hexadecyltrimethylammonium chloride. *Colloids Surf. A* **2014**, *460*, 28–37. [[CrossRef](#)]

18. Scheludko, A.; Platikanov, D. Untersuchung dünner flüssiger Schichten auf Quecksilber. *Kolloid Z.* **1961**, *175*, 150.
19. Mileva, E.; Tchoukov, P. Surfactant nanostructures in foam films. In *The Role of Surface Forces, Colloid and Interface Series*; Tadros, T., Ed.; Wiley-VCH: Weinheim, Germany, 2007; Volume 1, pp. 187–206.
20. Arabadzhieva, D.; Mileva, E.; Tchoukov, P.; Miller, R.; Ravera, F.; Liggieri, L. Adsorption layer properties and foam film drainage of aqueous solutions of tetraethyleneglycol monododecyl ether. *Colloids Surf. A* **2011**, *392*, 233–241. [[CrossRef](#)]
21. Arabadzhieva, D.; Soklev, B.; Mileva, E. Amphiphilic nanostructures in aqueous solutions of triethyleneglycol monododecyl ether. *Colloids Surf. A* **2013**, *419*, 194–200. [[CrossRef](#)]
22. Tchoukov, P.; Mileva, E.; Exerowa, D. Experimental evidences of self-assembly in foam films from amphiphilic solutions. *Langmuir* **2003**, *19*, 1215–1220. [[CrossRef](#)]
23. Kharitonova, T.V.; Ivanova, N.I.; Summ, B.D. Intermolecular interactions in the binary systems of cationic and nonionic surfactants. *Colloid J.* **2002**, *64*, 685–696.
24. Fainerman, V.B.; Miller, R.; Aksenenko, E.V. Simple model for prediction of surface tension of mixed surfactant solutions. *Adv. Colloid Interface Sci.* **2002**, *96*, 339–359. [[CrossRef](#)]
25. Javadian, S.; Gharibi, H.; Bromand, Z.; Sohrabi, B. Electrolyte effect on mixed micelle and interfacial properties of binary mixtures of cationic and nonionic surfactants. *J. Colloid Interface Sci.* **2008**, *318*, 449–456. [[CrossRef](#)] [[PubMed](#)]
26. Mhenga, A.; Zhaomin, L.; Chao, Z.; Gerald, G. Investigating synergism and antagonism of binary mixed surfactants for foam efficiency optimization in high salinity. *J. Pet. Sci. Eng.* **2019**, *175*, 489–494.
27. Hardy, E.; Holerca, M.; Ahmed, R.; Arvanitidou, E. Thickened Cationic and Nonionic Surfactant Cleansing Composition. U.S. Patent 10383808B2, 20 August 2019.
28. Hardy, E.; Holerca, M.; Ahmed, R.; Arvanitidou, E. Cleansing Composition Comprising a Nonionic/Cationic Surfactant Mixture. U.S. Patent 10772817B2, 15 September 2020.

**Publisher's Note:** MDPI stays neutral with regard to jurisdictional claims in published maps and institutional affiliations.



© 2020 by the authors. Licensee MDPI, Basel, Switzerland. This article is an open access article distributed under the terms and conditions of the Creative Commons Attribution (CC BY) license (<http://creativecommons.org/licenses/by/4.0/>).